Acta Crystallographica Section F
Structural Biology and Crystallization Communications
ISSN 1744-3091

Crystallization and diffraction analysis of thioredoxin reductase from *Streptomyces coelicolor*

Michaela Kohárýová,[a] Jiří Brynda,[b,c] Pavlína Řezáčová[b,c]* and Marta Kollárová[a]

[a]Faculty of Natural Sciences, Department of Biochemistry, Commenius University, Mlynská Dolina, 842 15 Bratislava, Slovakia, [b]Institute of Organic Chemistry and Biochemistry, Academy of Sciences of the Czech Republic, v.v.i., Flemingovo nám. 2, 16610 Praha 6, Czech Republic, and [c]Institute of Molecular Genetics, Academy of Sciences of the Czech Republic, v.v.i., Vídeňská 1083, 14220 Praha 4, Czech Republic

Correspondence e-mail: rezacova@uochb.cas.cz

Received 10 April 2011
Accepted 2 June 2011

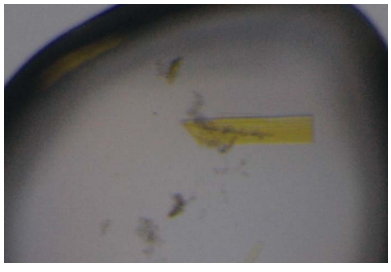

Thioredoxin reductases are homodimeric flavoenzymes that catalyze the transfer of electrons from NADPH to oxidized thioredoxin substrate. Bacterial thioredoxin reductases represent a promising target for the development of new antibiotics. Recombinant thioredoxin reductase TrxB from *Streptomyces coelicolor* was crystallized using the hanging-drop vapour-diffusion method. X-ray diffraction data were collected from cryocooled crystals to 2.4 Å resolution using a synchrotron-radiation source. The crystals belonged to the primitive monoclinic space group $P2_1$, with unit-cell parameters $a = 82.9$, $b = 60.6$, $c = 135.4$ Å, $\alpha = \gamma = 90.0$, $\beta = 96.5^\circ$.

1. Introduction

In most organisms, two essential redox systems are present inside the cell cytoplasm that are responsible for maintaining a redox balance: the thioredoxin and the glutathione/glutaredoxin systems (Holmgren, 1985; Gilbert, 1990; Williams, 1992). Similarly to other actinomycetes, including mycobacteria, the soil-dwelling Gram-positive bacterium *Streptomyces coelicolor* lacks the glutathione/glutaredoxin system and thus represents a good model organism for the study of redox regulation (Aharonowitz *et al.*, 1993; Newton *et al.*, 1996).

The thioredoxin system is formed by thioredoxin reductase (TrxR) and its characteristic substrate, the redox-active protein thioredoxin (Trx), the reduction of which takes place at the expense of NADPH. In most prokaryotic and eukaryotic organisms multiple functions are accomplished by a single Trx and a single TrxR. Interestingly, genome sequencing of *S. coelicolor* revealed the presence of several genes that possibly encode proteins of the thioredoxin system: three genes for thioredoxins (TrxA, TrxA2 and TrxA3), two genes for putative thioredoxins, one gene for thioredoxin reductase (TrxB) and two genes for putative thioredoxin reductases (Bentley *et al.*, 2000). It seems that *S. coelicolor* has a very complex redox system with a variety of reducing possibilities. This may also be responsible for the complex multicellular development of streptomycetes. Duplicated gene sets may represent 'tissue-specific' isoforms that operate in different phases of colonial development, a unique ability of this bacterium (Bentley *et al.*, 2002).

Thioredoxin reductases (EC 1.8.1.9) are physiologically important enzymes with properties (size, substrates, structure and mechanism of catalysis) that differ significantly between humans and bacteria. These differences allow bacterial TrxR to be used as a target for new antibiotics (Gromer *et al.*, 1998; Becker *et al.*, 2000; Hirt *et al.*, 2002). In some cases, inactivation or deletion of the gene encoding TrxR can cause lethality, as in Gram-positive *Staphylococcus aureus* (Uziel *et al.*, 2004). In efforts to find new drug targets in pathogens, many inhibitors are being tested for their ability to block thioredoxin reductases.

All TrxRs are members of the family of dimeric flavoenzymes, which catalyze the transfer of electrons between pyridine nucleotides and dithiol/disulfide compounds. Two distinct types of TrxR have evolved (Luthman & Holmgren, 1982). TrxRs isolated from *Plasmodium falciparum*, *Caenorhabditis elegans*, *Drosophila melanogaster* and higher eukaryotes, including mammals, have a

subunit with a molecular weight of 55 000. Mammalian TrxRs have a second redox-active site, a C-terminal -Cys-SeCys- (where SeCys is selenocysteine). Bacterial TrxRs and TrxRs isolated from lower species, including lower plants and fungi, have a subunit with a molecular weight of 35 000 which lacks a separate interface domain (Mustacich & Powis, 2000). Both types of TrxR are dimeric, with each monomer containing a flavin adenine dinucleotide (FAD) binding domain, a nicotinamide adenine dinucleotide phosphate (NADP) binding domain and an active site with a catalytic disulfide. Electrons from NADPH are transferred by the FAD prosthetic group to the redox-active disulfide and then to the thioredoxin substrate (Williams *et al.*, 2000).

The TrxB enzyme from *S. coelicolor* belongs to the low-molecular-weight thioredoxin reductases and shows 48% sequence identity to *Escherichia coli* TrxR and high identity to many other TrxRs. In order to understand the structure–function relationship and the mechanism of redox catalysis of TrxB from *S. coelicolor*, we initiated crystallographic analysis. Here, we report the crystallization and diffraction analysis of recombinant TrxB.

2. Materials and methods

2.1. Protein expression and purification

The preparation of the expression vector containing the gene for TrxB (GeneDB accession No. SCO3890) has previously been described by Štefanková *et al.* (2006). The expression vector carries a His_6-tag coding sequence at the N-terminal end of the target protein followed by a cleavage site for thrombin.

E. coli pLysS cell cultures were cultivated at 310 K in LB medium supplemented with 100 µg ml^{-1} ampicillin to an optical density ($OD_{600\,nm}$) of 0.5–0.7 at 600 nm. Overexpression of TrxB was induced by the addition of 1 m*M* isopropyl *β*-D-1-thiogalactopyranoside. After induction, the bacterial cultures were cultivated for 3 h. The bacterial cells were harvested by centrifugation, resuspended in a buffer consisting of 100 m*M* Tris–HCl pH 8.0 and 2 m*M* EDTA and disrupted by sonication using a Soniprep 150 (MSE, Crawley, England). Centrifugation at 39 000*g* for 20 min using a Beckman L8-50M/E ultracentrifuge (Beckman PA, California, USA) was carried out to remove cell debris.

The supernatant, which contained a mixture of soluble proteins, was applied onto an Ni^{2+}-chelating column (Novagen) equilibrated in a buffer consisting of 5 m*M* imidazole, 0.5 *M* NaCl and 20 m*M* Tris–HCl pH 7.9. Nonspecifically bound proteins were washed out with 60 m*M* imidazole and specifically bound His-tagged TrxB protein was eluted by increasing the imidazole concentration from 100 to 400 m*M*. The active fractions were pooled, concentrated to 100 mg ml^{-1} with an Amicon Ultra-4 ultrafiltration device, dialysed into storage buffer (20 m*M* Tris–HCl pH 8.0, 200 m*M* NaCl) and stored at 277 K.

2.2. Protein analyses

SDS–PAGE analyses were performed according to Laemmli (1970) using 12–15%(*w*/*v*) gels. The protein content was determined using the Coomassie Brilliant Blue binding method or by silver staining (Blum *et al.*, 1987). Protein concentration was determined by the Bradford assay (Bradford, 1976; Bio-Rad, Hercules, USA) using bovine serum albumin as a standard.

Analytical size-exclusion chromatography was performed on a Superdex 200 10/300 GL Tricorn column (Pharmacia) equilibrated in 20 m*M* Tris–HCl pH 8.0, 100 m*M* NaCl. A 90 µl protein sample at 26 mg ml^{-1} was analyzed and the molecular weight was estimated by comparison with protein standards (Sigma–Aldrich): blue dextran (2000 kDa), bovine serum albumin (66 kDa), carbonic anhydrase (29 kDa), cytochrome *c* (12.4 kDa) and aprotinin (6.5 kDa).

A spectrophotometric 5,5′-dithiobis-(2-nitrobenzoic acid) (DTNB) assay was used to quantify TrxR activity (Luthman & Holmgren, 1982). The enzymatic activity of TrxB was determined by following the reduction of DTNB by NADPH to yellow-coloured 5-thio-2-nitrobenzoic acid (TNB) at 412 nm.

Table 1
Data-collection statistics.

Values in parentheses are for the highest resolution shell.

No. of crystals	1
Beamline	MX14.2, BESSY
Wavelength (Å)	0.918
Detector	MAR Mosaic 225
Crystal-to-detector distance (mm)	250
Rotation range per image (°)	0.5
Total rotation range (°)	200
Exposure time per image (s)	6
Resolution range (Å)	50.00–2.40 (2.44–2.40)
Space group	$P2_1$
Unit-cell parameters (Å, °)	a = 82.9, b = 60.6, c = 135.4, $\alpha = \gamma$ = 90.0, β = 96.5
Total No. of measured intensities†	279104 (9115)
No. of unique reflections	56096 (2532)
Multiplicity	4.9 (3.6)
Average $I/\sigma(I)$	23.1 (2.8)
Completeness (%)	98.8 (90.1)
R_{merge}‡ (%)	6.3 (35.1)
Overall B factor from Wilson plot (Å^2)	43.4

† The criterion used for observed reflections was $I/\sigma(I) > 0$. ‡ $R_{merge} = 100 \times \sum_{hkl}\sum_i |I_i(hkl) - \langle I(hkl)\rangle| / \sum_{hkl}\sum_i I_i(hkl)$, where $I_i(hkl)$ is an individual intensity of the ith observation of reflection hkl and $\langle I(hkl)\rangle$ is the average intensity of reflection hkl with summation over all data.

2.3. Crystallization

TrxB at 28 mg ml^{-1} in 20 m*M* Tris–HCl pH 8.0, 200 m*M* NaCl buffer was used for crystallization experiments. A Pre-Crystallization Test (Hampton Research) was used to determine an appropriate protein concentration for crystallization screening. Initial crystallization trials were performed using the sitting-drop vapour-diffusion technique (Ducruix & Giegé, 1992) in an Intelli-Plate 96-3 with the help of a Gryphon crystallization workstation (Art Robbins Instruments, USA). The commercial JCSG+ Suite (Qiagen) was used for initial screening. Crystallization drops consisting of 0.4 µl protein solution and 0.4 µl reservoir solution were equilibrated against 150 µl reservoir solution.

Further optimization was performed by the hanging-drop vapour-diffusion method in 24-well NeXtal plates (Qiagen) with a 0.5 ml reservoir and drops consisting of 1 or 2 µl protein solution and 1 or 2 µl precipitant solution. Seeding techniques were used to improve the crystal quality. All crystallization experiments were performed at 293 K.

For analysis of the protein composition by SDS–PAGE, crystals were removed from the crystallization drop using a nylon loop and were dissolved in 5 µl water. Prior to their dissolution, crystals were washed twice for 30 s in 2 µl drops of reservoir solution.

2.4. Diffraction data collection and analysis

For data collection, crystals were mounted in a nylon loop and flash-cooled in liquid nitrogen. For cryoprotection, crystals were soaked for 3 s in reservoir solution supplemented with 20%(*v*/*v*) ethylene glycol.

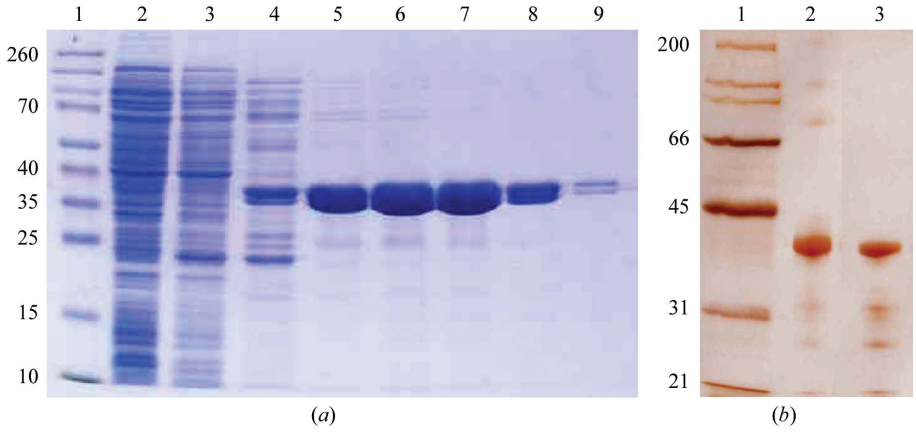

Figure 1
SDS–PAGE analyses of TrxB protein and crystals. (*a*) 15% SDS–PAGE gel stained with Coomassie Brilliant Blue R-250 following the isolation of *S. coelicolor* TrxB. Lane 1, molecular-weight standards (Fermentas; labelled in kDa); lane 2, cell extract loaded onto the Ni column; lane 3, flowthrough from the Ni column; lane 4, fraction washed from column by 60 m*M* imidazole; lanes 5–9, fractions eluted from Ni column by elution buffer (20 m*M* Tris–HCl pH 7.9, 0.5 *M* NaCl) supplemented with 0.1, 0.2, 0.3 and 1 *M* imidazole, respectively. Fractions 5–8 were pooled and used for crystallization. (*b*) 15% SDS–PAGE silver-stained gel of TrxB crystal. Lane 1, molecular-weight standards (Bio-Rad; labelled in kDa); lane 2, dissolved crystal of TrxB; lane 3, protein sample of TrxB used for crystallization experiments.

Diffraction data were collected on BESSY beamline MX14.2 with a 0.918 Å monochromatic fixed wavelength. A set of 400 images was recorded with a 0.5° oscillation angle, an exposure time of 6 s per image and a crystal-to-detector distance of 250 mm. The *HKL*-3000 suite (Minor *et al.*, 2006) was used for processing diffraction data. Data-collection statistics and crystal parameters are summarized in Table 1.

A self-rotation function was calculated by *MOLREP* (Vagin & Teplyakov, 2010) in the resolution range 50.0–3.5 Å; the integration radius was set to 15 Å.

3. Results

Thioredoxin reductase TrxB from *S. coelicolor* was expressed in *E. coli* and purified from a cytosolic fraction with a high yield of 53 mg protein from 1 l bacterial culture. The recombinant TrxB contained 322 amino-acid residues of its native sequence (SCO3890) and an N-terminal sequence consisting of six histidines and thrombin cleavage site (Leu-Val-Pro-Arg-Gly-Ser). The affinity tag was not removed from the protein and the His-tagged protein was used for crystallization.

The purity of the sample was confirmed by the presence of a major band on SDS–PAGE corresponding to a molecular weight of 34.9 kDa (Fig. 1). The molecular weight in solution was estimated by analytical gel chromatography to be 64.5 kDa and is consistent with the molecular weight of a TrxB homodimer. The biological activity of recombinant TrxB was confirmed by a DTNB assay. The structural homogeneity was also confirmed by dynamic light-scattering analysis (data not shown).

Initial protein crystals were obtained by vapour diffusion in sitting-drop mode using solutions from the JCSG+ Suite crystallization screen (Quiagen). Needle-shaped and plate-like crystals of yellow colour were obtained within 20 d at 293 K in a condition consisting of 0.1 *M* Bis-Tris pH 5.5, 0.2 *M* lithium sulfate and 25%(*w*/*v*) PEG 3350. The distinct yellow colour of the crystals was caused by the presence of a flavin adenine dinucleotide (FAD) cofactor in the enzyme, which naturally co-purified with the recombinant enzyme.

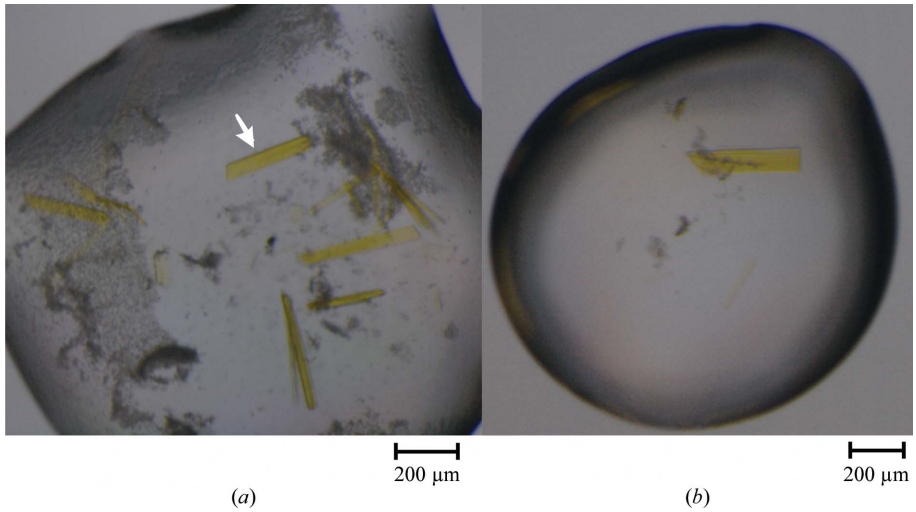

Figure 2
(*a*) Crystals of TrxB in visible light grown in 90 m*M* Bis-Tris pH 5.5, 180 m*M* lithium sulfate and 22.5% PEG 3350. (*b*) The crystal used for diffraction data collection was obtained by macroseeding of a crystal from the original drop [marked with an arrow in (*a*)] to a new drop containing diluted precipitant solution [80 m*M* Bis-Tris pH 5.5, 160 m*M* lithium sulfate and 20%(*w*/*v*) PEG].

Further optimization of crystallization conditions was performed with larger volumes using the hanging-drop mode. Optimization by lowering the precipitant concentration and varying the protein: precipitant ratio in the crystallization drops to 1:2 led to the production of larger plate-like crystals with dimensions of about 291 × 57 × 10 µm. To increase the crystal size, macroseeding was used. Crystals grown in a condition consisting of 90 m*M* Bis-Tris pH 5.5, 180 m*M* lithium sulfate and 22.5%(*w*/*v*) PEG 3350 were transferred to a condition containing a lower precipitant concentration [80 m*M* Bis-Tris pH 5.5, 160 m*M* lithium sulfate and 20%(*w*/*v*) PEG]. The crystals reached their final size of 400 × 80 × 10 µm within 7 d (Fig. 2). Analysis of their content was performed by SDS–PAGE of the dissolved crystals. This analysis confirmed that crystals of full-length TrxB were formed, as the protein composition of the crystals was very similar to that observed in the protein solution used for crystallization (Fig. 2).

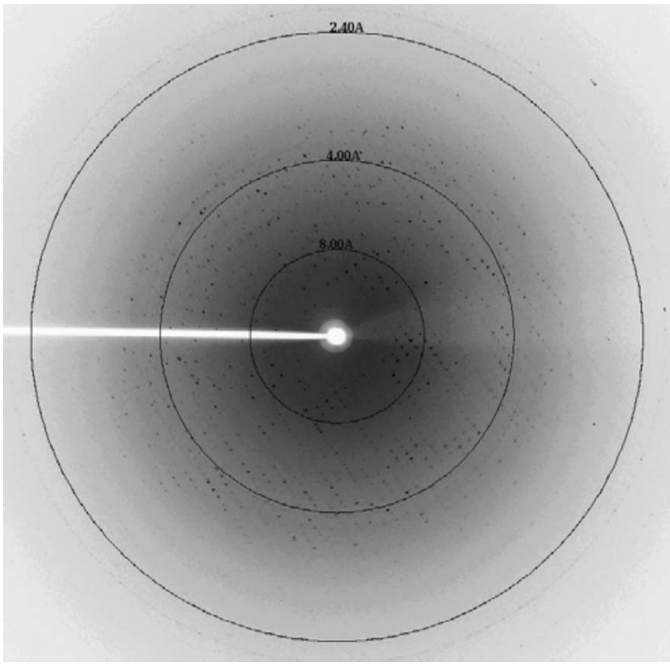

Figure 3
Diffraction image from a TrxB crystal.

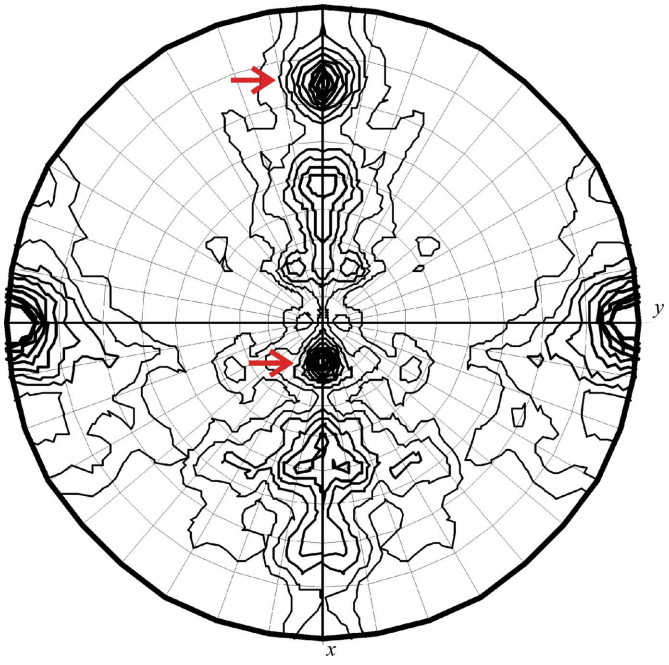

Figure 4
A self-rotation function map of TrxB diffraction data plotted at $\chi = 180^\circ$. The grid lines are drawn at 10° intervals. The noncrystallographic twofold axes are indicated by red arrows.

For diffraction measurements, crystals were cryocooled in mother liquor supplemented with 20%(*v*/*v*) ethylene glycol as a cryoprotectant and used to collect a complete data set to 2.4 Å resolution at 100 K at the BESSY synchrotron (beamline MX14.2; Fig. 3). The crystals belonged to space group $P2_1$, with unit-cell parameters $a = 82.9$, $b = 60.6$, $c = 135.4$ Å, $\alpha = \gamma = 90.0$, $\beta = 96.5^\circ$ (Table 1). Owing to the plate-like crystal shape, the crystals exhibited anisotropic diffraction to a minimum Bragg spacing ($d_{\rm min}$) of about 2.3 Å in one direction and to a $d_{\rm min}$ of about 2.9 Å in the other direction. The low value of the completeness in the highest resolution shell is a consequence of this anisotropy. The extent of radiation damage during data collection was monitored by the increase in scaling *B* factor. Radiation damage was not obvious as the *B* factor during scaling of the diffraction images did not exceed 6.0 Å^2.

An evaluation of the crystal-packing parameters indicated the presence of four molecules in the asymmetric unit, with a Matthews coefficient of 2.74 Å^3 Da^{-1} and a corresponding solvent content of 50% (Matthews, 1968). A self-rotation function indicated the presence of two noncrystallographic twofold axes perpendicular to the crystallographic 2_1 axis (Fig. 4). As a stable dimer was observed for TrxB, it is likely that the asymmetric unit contains two dimeric biologically active units.

The diffraction data will be used to determine the structure of TrxB by molecular replacement using the available structures of the homologous enzymes *Mycobacterium tuberculosis* TrxR (Akif *et al.*, 2005; 62% sequence identity), *E. coli* TrxR (Lennon *et al.*, 1999; 48% sequence similarity) and barley thioredoxin reductase 2 (Kirkensgaard *et al.*, 2009; 53% sequence similarity).

This contribution is a result of the implementation of the 'Centre of Excellence for Exploitation of Informational Biomacromolecules for Improvement of Quality of Life' project supported by the Research and Development Operational Programme funded by the ERDF (Contract No. ITMS 26240120027) and VEGA 1/0371/09 'Study of Thioredoxin System Components in *Streptomyces*'. This work was also supported by projects Z40550506 and Z50520514 awarded by the Academy of Sciences of the Czech Republic. Diffraction data were collected on beamline MX14.2 at BESSY, Berlin, Germany. The authors wish to thank Devon Maloy for critical proofreading of the manuscript.

References

Aharonowitz, Y., Av-Gay, Y., Schreiber, R. & Cohen, G. (1993). *J. Bacteriol.* **175**, 623–629.
Akif, M., Suhre, K., Verma, C. & Mande, S. C. (2005). *Acta Cryst.* D**61**, 1603–1611.
Becker, K., Gromer, S., Schirmer, R. H. & Müller, S. (2000). *Eur. J. Biochem.* **267**, 6118–6125.
Bentley, S. D. *et al.* (2002). *Nature (London)*, **417**, 141–147.
Blum, H., Beier, H. & Gross, H. J. (1987). *Electrophoresis*, **8**, 93–99.
Bradford, M. M. (1976). *Anal. Biochem.* **72**, 248–254.
Ducruix, A. & Giegé, R. (1992). *Crystallization of Nucleic Acids and Proteins: A Practical Approach.* Oxford University Press.
Gilbert, H. F. (1990). *Adv. Enzymol. Relat. Areas Mol. Biol.* **63**, 69–172.

Gromer, S., Wissing, J., Behne, D., Ashman, K., Schirmer, R. H., Flohé, L. & Becker, K. (1998). *Biochem. J.* **332**, 591–592.
Hirt, R. P., Müller, S., Embley, T. M. & Coombs, G. H. (2002). *Trends Parasitol.* **18**, 302–308.
Holmgren, A. (1985). *Annu. Rev. Biochem.* **54**, 237–271.
Kirkensgaard, K. G., Hägglund, P., Finnie, C., Svensson, B. & Henriksen, A. (2009). *Acta Cryst.* D**65**, 932–941.
Laemmli, U. K. (1970). *Nature (London)*, **227**, 680–685.
Lennon, B. W., Williams, C. H. Jr & Ludwig, M. L. (1999). *Protein Sci.* **8**, 2366–2379.
Luthman, M. & Holmgren, A. (1982). *Biochemistry*, **21**, 6628–6633.
Matthews, B. W. (1968). *J. Mol. Biol.* **33**, 491–497.
Minor, W., Cymborowski, M., Otwinowski, Z. & Chruszcz, M. (2006). *Acta Cryst.* D**62**, 859–866.
Mustacich, D. & Powis, G. (2000). *Biochem. J.* **346**, 1–8.
Newton, G. L., Arnold, K., Price, M. S., Sherrill, C., Delcardayre, S. B., Aharonowitz, Y., Cohen, G., Davies, J., Fahey, R. C. & Davis, C. (1996). *J. Bacteriol.* **178**, 1990–1995.
Štefanková, P., Perečko, D., Barák, I. & Kollárová, M. (2006). *J. Basic Microbiol.* **46**, 47–55.
Uziel, O., Borovok, I., Schreiber, R., Cohen, G. & Aharonowitz, Y. (2004). *J. Bacteriol.* **186**, 326–334.
Vagin, A. & Teplyakov, A. (2010). *Acta Cryst.* D**66**, 22–25.
Williams, C. H. Jr (1992). *Chemistry and Biochemistry of Flavoenzymes*, edited by F. Müller, pp. 121–211. Boca Raton: CRC Press.
Williams, C. H. Jr, Arscott, L. D., Müller, S., Lennon, B. W., Ludwig, M. L., Wang, P.-F., Veine, D. M., Becker, K. & Schirmer, R. H. (2000). *Eur. J. Biochem.* **267**, 6110–6117.